

# Conductive electron heat flow along magnetic field lines

E. D. Held<sup>a)</sup>

*Los Alamos National Laboratory, Los Alamos, New Mexico 87545*

J. D. Callen and C. C. Hegna

*Physics and Engineering Physics Departments, University of Wisconsin, Madison, Wisconsin 53706*

C. R. Sovinec

*Los Alamos National Laboratory, Los Alamos, New Mexico 87545*

(Received 18 July 2000; accepted 19 December 2000)

In this work, a unified closure for the conductive electron heat flux along magnetic field lines is derived and examined. Both free-streaming and collisional pitch-angle scattering of electrons are present in the drift kinetic equation which is solved using an expansion in pitch-angle eigenfunctions (Legendre polynomials). The closure takes the form of a generic integral operator involving the electron temperature variation along a magnetic field line and the electron speed. Derived for arbitrary collisionality, the heat flux closure may be written in forms resembling previous collisional and collisionless expressions. Electrons with two to three times the thermal speed are shown to carry heat for all collisionalities and thermal electrons make an important contribution to the heat flow in regimes of moderate to low collisionality. As a practical application, the flow of electron heat along a chaotic magnetic field is calculated in order to highlight the nonlocal nature of the closure which allows for heat to flow against local temperature gradients. © 2001 American Institute of Physics. [DOI: 10.1063/1.1349876]

## I. INTRODUCTION

For many plasmas of interest, electron heat transport along magnetic field lines is complicated by the fact that collisional mean free paths are often comparable to or much longer than gradient scale lengths. In order to model heat flow effects in these moderately collisional to nearly collisionless plasmas, collisional effects should be included in the analysis without moving entirely to the collisional limit. With this in mind, we develop a general analytic closure for the parallel electron heat flux derived for arbitrary collisionality. This closure takes the form of an integral operator involving the electron temperature variation along a magnetic field line and the electron speed.

The initial expression for the parallel heat flux in the collision-dominated regime is due to Braginskii<sup>1</sup> who derived the following diffusive flux for an electron/proton plasma:

$$q_{\parallel} = -3.16 \left( \frac{n_e T_e \tau_e}{m_e} \right) \nabla_{\parallel} T_e, \quad (1)$$

where  $n_e$ ,  $T_e$ ,  $\tau_e$ , and  $m_e$  are the electron density, temperature, collision time, and mass, respectively. Since many astrophysical plasmas and present-day, high-temperature magnetic fusion experiments are in a regime where collisions are infrequent, there have been attempts to calculate the heat flux in the collisionless limit as well. In particular, Hammett and Perkins<sup>2</sup> propose a collisionless heat flux characterized by free-streaming of electrons along magnetic field lines. The

form for the collisionless closure that will be referenced in this work is set forth by Snyder *et al.* in their 3+1 moment model,<sup>3</sup> where it is assumed that the lowest-order distribution function is a bi-Maxwellian parameterized by parallel and perpendicular electron temperatures. If the parallel and perpendicular electron temperatures are assumed to be equal, this closure may be written as

$$q_{\parallel}(L') = \frac{n_e v_{\text{the}}}{\pi^{3/2}} \int_0^{\infty} dL \frac{T_e(L' - L) - T_e(L' + L)}{L/2}, \quad (2)$$

where  $v_{\text{the}} = \sqrt{2T_e/m_e}$  is the electron thermal speed and  $L$  is the coordinate along the magnetic field.

The collisional and collisionless limits are interpreted as involving very different physics, namely diffusion in the collisional regime and free-streaming in the collisionless limit. The closure derived in this work unifies these physical processes allowing for a continuous variation when going from the collisional to the nearly collisionless regime. A previous author<sup>4,5</sup> has derived a general spectral form for the parallel heat flow that reduces to the collisional and collisionless results when the appropriate limits are taken. Nevertheless, it remains difficult to gain insight from the spectral closure in regimes of moderate collisionality when the Fourier-space representation of thermodynamic forces is difficult to ascertain. Such is the case when electromagnetic perturbations with complex Fourier spectra are the cause of electron heat flow along magnetic field lines. One example of when a real-space, electromagnetic closure may prove useful involves electron heat flowing along a resistively evolving, chaotic magnetic field. This represents a dominant process for galaxy cluster cooling flows<sup>6</sup> and in the core of reversed field

<sup>a)</sup>Present address: Physics Department, Utah State University, Logan, Utah 84322-4415. Electronic mail: eheld@cc.usu.edu

pinches (RFP's).<sup>7</sup> A second example prevalent in toroidal confinement devices involves the flattening of electron temperature inside helical magnetic islands due to electron heat flow along field lines.<sup>8</sup>

Furthermore, previous work<sup>3-5</sup> attempts to generalize the collisional and collisionless closures using a Bhatnagar-Gross-Krook (BGK) collision operator.<sup>9</sup> In kinetic studies of heat flow, however, a more relevant collisional mechanism involves the scattering of an electron's parallel velocity in pitch-angle,  $\xi = v_{\parallel}/v$ , where  $v_{\parallel}$  is the parallel component of the guiding center motion and  $v$  is the speed. Unlike the BGK operator, the speed-dependent, pitch-angle scattering (Lorentz) operator permits a discussion of the energy weighting of heat-flow-carrying electrons similar to that presented in work by Krasheninnikov.<sup>10</sup> In addition, the Lorentz operator allows for trapped particle effects when variations in  $|B|$  along a magnetic field line become important. The generalization of the pitch-angle scattering operator and its effects on parallel heat flow for an inhomogeneous magnetic field will be discussed in subsequent work.

In this work, a Chapman-Enskog-type (CEL) approach is adopted.<sup>11-13</sup> The distribution function,  $f_e$ , is written as a Maxwellian parameterized by the lowest-order, even fluid moments,  $n_e$  and  $T_e$ , plus an additional kinetic distortion,  $F_e$ ,<sup>14</sup>

$$f_e = f_{Me} + F_e = n_e(\mathbf{x}, t) \left[ \frac{m}{2\pi T_e(\mathbf{x}, t)} \right]^{3/2} \times \exp \left[ -\frac{m_e v^2}{2T_e(\mathbf{x}, t)} \right] + F_e, \quad (3)$$

where an extended drift ordering is employed and  $F_e$  is considered small compared to  $f_{Me}$ . Similar but more complex ansatz are used in previous work where either the flow<sup>11,12</sup> or the flow and heat flow<sup>13</sup> are incorporated into the parameterization of  $f_{Me}$ . There a rigorous moment approach is employed for a more complete closure scheme. Here the emphasis is on deriving a general form for the conductive, parallel electron heat flow only and the CEL approach is employed since it makes explicit the fact that parallel gradients in the thermodynamic variables that parameterize the Maxwellian are the dominant cause of parallel heat flow.

This paper is organized as follows. In Sec. II, the kinetic equation of interest is formulated by substituting the ansatz in Eq. (3) into a simplified electron drift kinetic equation (DKE). In Sec. III, the time-independent DKE is solved and the heat flux closure is constructed and shown to agree qualitatively with previous collisional and collisionless expressions. The quantitative aspects of the closure are investigated in Sec. IV, where the heat flux for a sinusoidal temperature perturbation is examined as collisionality varies. In Sec. V, we present a sample calculation of an effective, cross-field thermal diffusivity due to electron heat flow along a chaotic magnetic field and in Sec. VI we summarize the important results.

## II. SIMPLIFIED ELECTRON DRIFT KINETIC EQUATION

In order to make clear the assumptions included in the heat flux closure derived here we begin by writing the full electron drift kinetic equation (DKE) as follows:<sup>15</sup>

$$\frac{\partial f_e}{\partial t} + (\mathbf{v}_{\parallel} + \mathbf{v}_D) \cdot \nabla f_e + \left[ \frac{\mu}{m\nu} \frac{\partial B}{\partial t} + \frac{e}{m_e \nu} (\mathbf{v}_{\parallel} + \mathbf{v}_D) \cdot \mathbf{E} \right] \frac{\partial f_e}{\partial v} = C(f_e). \quad (4)$$

Here  $\mathbf{v}_D$  is the perpendicular component of the guiding center motion,  $\mu$  is the magnetic moment, and the collision operator,  $C(f_e)$ , represents Coulomb collision events. This equation describes the evolution of a distribution of electron guiding center orbits, i.e., gyromotion has been averaged out of the equation.

We begin by applying an extended drift ordering to Eq. (4), namely,  $(\mathbf{v}_D \cdot \nabla)/(\mathbf{v}_{\parallel} \cdot \nabla) \sim \delta$  and  $(\mathbf{v}_D \cdot \mathbf{E})/(\mathbf{v}_{\parallel} \cdot \mathbf{E}) \sim \delta$ . This implies that the lowest-order guiding center trajectories coincide exactly with magnetic field lines. Furthermore, for the higher-order heat flow moment, we make the common assumption that the flow of electron heat does not lead to significant charge imbalance along magnetic field lines, i.e.,  $eL\nabla_{\parallel}\phi/T_e \sim \delta$ , where  $\nabla_{\parallel}\phi$  is the electrostatic portion of the parallel electric field and  $L$  is a typical parallel scale length. Note, however, that this assumption is inappropriate for the lower-order flow moment. Because quasineutrality enters to lowest order, a steady-state solution of the electron DKE without the electric field term has little to say about the flow of electrons along magnetic field lines. For this reason, no attempt is made here to calculate the parallel electron flow.

In Refs. 4 and 5, sources of particles and energy are used in the DKE to explain the existence of gradients and hence transport along the magnetic field in the time-asymptotic limit. Here we take the standard approach of attempting to write closures in terms of thermodynamic forces without worrying about the sources giving rise to thermodynamic gradients. This approach is consistent with gradients along the magnetic field that result from other causes such as the resistive evolution of a magnetic field in the presence of cross field gradients. In most cases of interest, it may be assumed that the resistive time is long compared to the transit and collision times, hence,  $(\tau_e/B)(\partial B/\partial t) \sim \delta$ . Note that the magnetic field still manifests itself spatially in the free-streaming operator,  $\mathbf{v}_{\parallel} \cdot \nabla$ . Based on these simplifications, the order  $\delta^0$  DKE becomes

$$\frac{\partial f_e^0}{\partial t} + \mathbf{v}_{\parallel} \cdot \nabla f_e^0 = C(f_e^0). \quad (5)$$

This equation balances free-streaming along field lines with collisional and time-dependent effects.

In order to solve Eq. (5), we substitute the ansatz in Eq. (3) for  $f_e^0$ ,

$$\left( \frac{\partial}{\partial t} + \mathbf{v}_{\parallel} \cdot \nabla \right) F - C(F) = - \left( \frac{\partial}{\partial t} + \mathbf{v}_{\parallel} \cdot \nabla \right) f_M, \quad (6)$$

where the  $e$  subscript is dropped heretofore. An essential aspect of the ansatz in Eq. (3) is that it assumes small departures from a Maxwellian, i.e.,  $F/f_M \ll 1$ . Note that the ab-

sence of the electron flow,  $\mathbf{V}_e$ , in  $f_M$  implies that the Maxwellian is nearly stationary such that  $v$  represents the random guiding center speed. Equation (6) makes clear the fact that it is variations in  $f_M$  that drive the kinetic distortion  $F$  and hence produce a finite heat flow moment. Higher order effects due to the free-streaming operator,  $\mathbf{v}_\parallel \cdot \nabla$ , can in principle be incorporated into the heat flux closure by including the full (unexpanded) Maxwellian on the right-hand side of Eq. (6). This incorporates the combined effects of perturbed density and temperature and allows for collisional effects to vary along magnetic field lines. Note, however, that this approach is approximate since it ignores the corrections due to finite drift effects that would alter higher-order terms in  $F$ . Later,  $f_M$  in Eq. (6) will be expanded explicitly according to the modified drift ordering in order to simplify the velocity-space integration and to permit comparison with previous heat flux closures.

At this point we discuss the form for the collision operator,  $C(F)$ , in Eq. (6). Because the scattering of directed momentum due to multiple small-angle Coulomb collisions is important in studies of heat flow, we introduce the following form for the collision operator,  $C(F) = (L_{ei} + L_{ee})F$ . The Lorentz scattering operator,  $L_{ej}$ , converted from spherical velocity space to the pitch angle variable,  $\xi = \pm \sqrt{1 - v_\perp^2/v^2}$ , is

$$L_{ej} = v_{\perp ej}(v) \frac{\partial}{\partial \xi} (1 - \xi^2) \frac{\partial}{\partial \xi}, \tag{7}$$

where  $\xi$  varies from  $\xi=0$  for an electron with all of its energy devoted to gyromotion to  $\xi = \pm 1$  for an electron with no magnetic moment.

Because we have an interest in investigating the energy weighting of heat-flow-carrying electrons, we employ the following rigorous form for the collision frequency representing perpendicular diffusion of a test electron scattering off a background Maxwellian,

$$v_{\perp ej}(v) = \frac{v_{ej}}{2} \left( \frac{v_{\text{the}}}{v} \right)^3 \left[ \Phi \left( \frac{v}{v_{thj}} \right) - G \left( \frac{v}{v_{thj}} \right) \right], \tag{8}$$

where  $\Phi$  is the error function and  $G = (v_{thj}/v)^2 (\Phi - (v/v_{thj})\Phi')/2$ . The reference collision frequency is  $v_{ej} = 4\pi n_j e^2 e_j^2 \ln \Lambda_{ej} / (m_e^2 v_{\text{the}}^3)$ . A simplification of the electron/ion collision frequency is in order so long as  $v_{\text{the}}/v_{thi} > \sqrt{m_e/m_i}$ . In this limit the relevant collision frequency becomes

$$\bar{v} = v_{\perp ei} + v_{\perp ee} = \frac{v_{ee}}{2s^3} [Z_{\text{eff}} + \Phi(s) - G(s)], \tag{9}$$

where the speed variable  $s = v/v_{\text{the}}$  and  $Z_{\text{eff}} = \sum_j n_j Z_j^2 / \sum_j n_j Z_j$ , with the sum performed over all ion species. Note that the linear collision operator in Eq. (7) does not include the momentum restoring corrections that enter at order  $V_{\parallel e}/v_{\text{the}}$  and  $V_{\parallel i}/v_{\text{the}}$ , where  $V_{\parallel e}$  and  $V_{\parallel i}$  are the parallel electron and ion flows.

Equation (6) may now be written in terms of the variables  $\xi$  and  $v$  as

$$\begin{aligned} & \left( \frac{\partial}{\partial t} + v \xi \frac{\partial}{\partial L'} - \bar{v} \frac{\partial}{\partial \xi} (1 - \xi^2) \frac{\partial}{\partial \xi} \right) F \\ & = - \left( \frac{\partial}{\partial t} + v \xi \frac{\partial}{\partial L'} \right) f_M, \end{aligned} \tag{10}$$

where  $L'$  is the coordinate along the magnetic field. Note that Eq. (10) is complicated by the fact that it is not separable in the pitch-angle variable due to free-streaming over gradients in  $F$  and  $f_M$ . Since the eigenfunctions of the Lorentz scattering operator are Legendre polynomials, we expand the kinetic distortion as  $F = \sum_{n=0}^N F_n(L, t, v) P_n(\xi)$  such that  $L(F) = -\sum \lambda_n F_n P_n$ , where  $\lambda_n = n(n+1)$ . Substituting into Eq. (10) and applying orthogonality yields a set of  $N+1$  equations for the coefficients,  $F_n$ ,

$$\begin{aligned} & \frac{1}{v} \left( \frac{\partial}{\partial t} + \bar{v} \lambda_n \right) F_n + \sum_{n'=n-1, n+1} \langle \rangle_{n, n'} \frac{\partial F_{n'}}{\partial L'} \\ & = - \left( \frac{\delta_{n,0}}{v} \frac{\partial}{\partial t} + \delta_{n,1} \langle \rangle_{n,0} \frac{\partial}{\partial L'} \right) f_M, \end{aligned} \tag{11}$$

where

$$\langle \rangle_{n, n'} = \frac{\int_{-1}^1 d\xi \xi P_n P_{n'}}{\int_{-1}^1 d\xi P_n^2}, \tag{12}$$

and  $\delta_{n, n'}$  is the Kronecker delta.

### III. GENERAL HEAT FLUX

In this section a general heat flux is constructed and written in forms resembling Eqs. (1) and (2). In the interest of presenting a simplified solution, we drop the time dependence in Eq. (11). This requires ignoring the  $n=0$  equation since in the time-asymptotic, Lorentz-scattering-only limit, nothing gives rise to a non-Maxwellian, pitch-angle-independent distribution function. Starting with  $n=1$  prevents the problem of having too many equations with too few unknowns (the qualitative error in low collisionality regimes that results from this approximation will be addressed in future work where finite time dependence is retained). Furthermore, orthogonality between the Legendre polynomials means that by starting with  $P_1$ , the expansion trivially conserves  $n$  and  $T [\int d^3 v F = 0$  and  $\int d^3 v (s^2 - (1/2)) F = 0]$ , as required by the Chapman-Enskog ansatz. Inspection of Eq. (11) shows that the time-independent system is equivalent to  $\mathbf{A}\mathbf{f} = \mathbf{g}$ , where  $\mathbf{A}$  is a block tridiagonal differential operator acting on the solution vector,  $\mathbf{f}$ , whose elements are the coefficients of the expansion in Legendre polynomials. The inhomogeneous vector,  $\mathbf{g}$ , has as its only nonzero entry the second term on the right-hand side of Eq. (11),  $\mathbf{g}(1) = \mathbf{g} = -\langle \rangle_{1,0} \partial f_M / \partial L'$ .

In order to solve this system, we begin by substituting in trial solution vectors of the form  $\mathbf{f}_i = \mathbf{c}_i \exp(\int L' d\bar{L} \bar{k}_i)$ , where

$$\bar{k}_i(s) = \frac{k_i}{2L_{mf} p s^4} (Z_{\text{eff}} + \Phi(s) - G(s)), \tag{13}$$

and the mean free path,  $L_{\text{mfp}} = v_{\text{the}} / \nu_{ee}$ . Here the  $N \bar{k}_i$ 's, which come in positive–negative pairs, have dimensions of inverse length such that  $\bar{k}_i^{-1}$  may be thought of as a speed-dependent, effective collisional mean free path. The  $N$  elements of vector  $\mathbf{c}_i$  are associated with the  $N$  coefficients,  $F_n$ , and are for the moment undetermined constants. Upon differentiation with respect to  $L'$ , the trial solution converts the homogeneous system of  $N$  coupled differential equations ( $\mathbf{A}\mathbf{f}=\mathbf{0}$ ) into a purely algebraic system of the form  $\bar{\mathbf{A}}(k_i)\mathbf{c}_i = \mathbf{0}$ . For small sets of equations the  $N k_i$ 's may be determined as the roots of the characteristic polynomial generated by inverting  $\bar{\mathbf{A}}$ . In the interest of accuracy, however, for large sets of equations the roots should be determined via some other procedure. One method converges on  $k_i$  iteratively using Newton's method where  $k_i$  is adjusted until the matrix  $\bar{\mathbf{A}}$  is singular, i.e., one of its eigenvalues is zero. After determining  $k_i$ , the associated eigenvector,  $\mathbf{c}_i$ , which corresponds to one vector in the nullspace of  $\bar{\mathbf{A}}$ , may be easily determined from the singular value decomposition of  $\bar{\mathbf{A}}$ .<sup>16</sup> The sum of the  $N$  trial solution vectors form the characteristic (homogeneous) solution of the original system of equations.

For the inhomogeneous system, similar trial solutions of the form  $\mathbf{g}_i = d_i \mathbf{c}_i \int^{L'} dL'' g(L'') \exp(-\int_{L'}^{L''} d\bar{L} \bar{k}_i)$  may be inserted into Eq. (11) and the constants  $d_i$  may again be determined via linear algebra. The complete solution of the inhomogeneous system becomes

$$F_n(s, \xi, L') = \sum_{i=1}^N \left[ b_i c_{ni} \exp\left(\int^{L'} d\bar{L} \bar{k}_i\right) + a_{ni} \int^{L'} dL'' g(L'') \exp\left(-\int_{L'}^{L''} d\bar{L} \bar{k}_i\right) \right], \tag{14}$$

where  $a_{ni} = d_i c_{in}$ . For the kinetic distortion to remain well-behaved as  $L' \rightarrow \pm\infty$ , it must be the case that the coefficients of the characteristic solution vanish, i.e.,  $b_i = 0$ . Likewise, it is necessary to choose the limits of the field line integration in accordance with the sign of  $\bar{k}_i$ . Taking this into consideration, we transform to the variable,  $L = L'' - L'$ , in order to write the following general solution for  $F$ ,

$$F(s, \xi, L') = \sum_{n=1}^N P_n \sum_{\bar{k}_i > 0} a_{ni} \int_0^\infty dL (g(L'+L) + g(L'-L)) \exp\left(-\int_0^L d\bar{L} \bar{k}_i\right), \tag{15}$$

where the second sum is performed over the  $N/2$  positive  $\bar{k}_i$ 's.

We now define the parallel conductive heat flux as

$$q_{\parallel} \equiv -T \int d^3v L_1^{(3/2)}(s) v_{\parallel} F, \tag{16}$$

where the Laguerre polynomial  $L_1^{(3/2)}(s) = 5/2 - s^2$ . Here we have multiplied by  $-TL_1^{(3/2)}$  instead of simply by  $Ts^2$  in order to subtract off the contribution to the heat flow coming

from any finite electron flow moment. This implies that we are only interested in the flow of heat due to the random parallel velocities in the moving frame of the electron fluid. Note that the presence of  $v_{\parallel} = v\xi$  in Eq. (16) implies that only  $P_1$  in the Legendre polynomial expansion contributes directly to the parallel heat flow based on orthogonality. Substituting Eq. (15) into the above definition of the heat flux results in a double integral over  $L$  and  $s$ ,

$$q_{\parallel}(L') = -\frac{4\pi}{3} \int_0^\infty dL \int_0^\infty dv v^3 L_1^{(3/2)} \frac{\partial}{\partial L} [f_M(L'+L) + f_M(L'-L)] \sum_{\bar{k}_i > 0} |a_{1i}| \exp\left(-\int_0^L d\bar{L} \bar{k}_i\right), \tag{17}$$

where the integrations over pitch-angle and gyroangle have been performed. Here we can make the thermodynamic drives explicit by writing  $\partial f_M / \partial L$  in terms of pressure,  $p = nT$ , and  $T$ ,

$$\frac{\partial f_M}{\partial L} = f_M \frac{\partial}{\partial L} (\ln p + L_1^{(3/2)} \ln T). \tag{18}$$

In order to relate the heat flux closure in Eq. (17) to previous expressions, a few simplifications are required. In collisional Chapman–Enskog theory, orthogonality among Laguerre polynomials dictates that only the gradient in temperature contributes to the conductive heat flow moment defined in Eq. (16). In general, however, the speed dependence present in the  $\bar{k}_i$ 's means that both  $p$  and  $T$  contribute to the heat flux. In the interest of comparing with previous expressions, however, we will only consider the conductive heat flux that arises from temperature variations along magnetic field lines, i.e.,  $\partial f_M / \partial L$  in Eq. (18) becomes just  $f_M L_1^{(3/2)} \partial(\ln T) / \partial L$ . Note that the full Maxwellian,  $f_M$ , still weights the temperature variations along a field line and therefore incorporates approximate nonlinearities into the closure by allowing both density and temperature to vary simultaneously. As a further simplification of Eq. (17), we let  $f_M$  in  $f_M L_1^{(3/2)} \partial(\ln T) / \partial L$  take the form of a spatially constant Maxwellian,  $f_M^{\text{eq}} = (n^{\text{eq}} / \pi^{3/2} v_{\text{the}}^3) e^{-s^2}$ , such that our drive term for the heat flux becomes the lowest-order term in our modified drift-ordered expansion. Based on these assumptions, the heat flux may be written,

$$q_{\parallel}(L') = -\frac{n^{\text{eq}} v_{\text{the}}}{\pi^{3/2}} \int_0^\infty dL \left[ \frac{\partial T(L'+L)}{\partial L} + \frac{\partial T(L'-L)}{\partial L} \right] K(L), \tag{19}$$

where

$$K(L) = \frac{4\pi}{3} \int_0^\infty ds \left( s^2 - \frac{5}{2} \right)^2 s^3 \times \sum_{\bar{k}_i > 0} |a_{1i}| \exp\left(-s^2 - \int_0^L d\bar{L} \bar{k}_i\right). \tag{20}$$

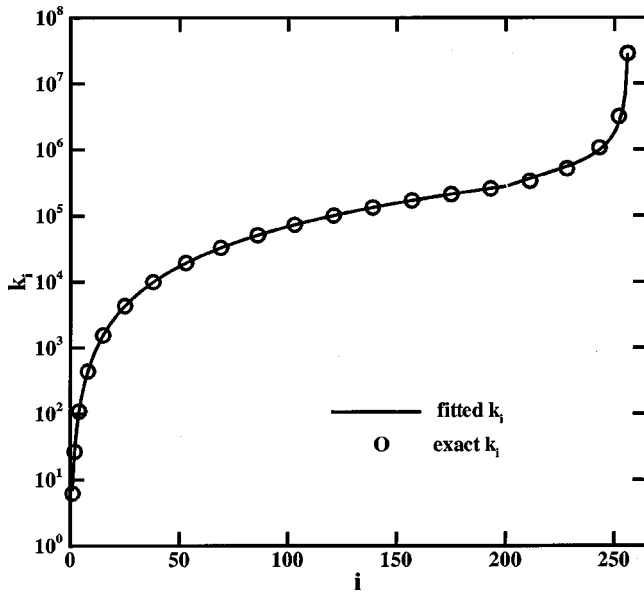


FIG. 1. Positive  $k_i$ 's resulting from an expansion of the kinetic distortion,  $F$ , in a basis of 512 Legendre polynomials. Approximate  $k_i$ 's may be generated using the following parameterizations:  $k_{1-200} = 6.76i^{2.004}$  and  $k_{201-256} = 2.82 \times 10^5 (1.0 - \tan[0.02838(201 - i)])$ .

Figures 1 and 2 show the positive  $k_i$  and  $a_{1,i}$  for  $N=512$ . Approximate values for the roots and coefficients may be obtained using the parameterizations given in the figure captions.

At this point we wish to touch base with the qualitative aspects of the collisional and collisionless expressions in Eqs. (1) and (2). We begin by defining the collisional limit as the regime in which the heat flux in Eq. (19) converges in a distance  $L$  over which  $\partial T/\partial L$  may be considered constant. Furthermore, since it will be shown later that higher-energy

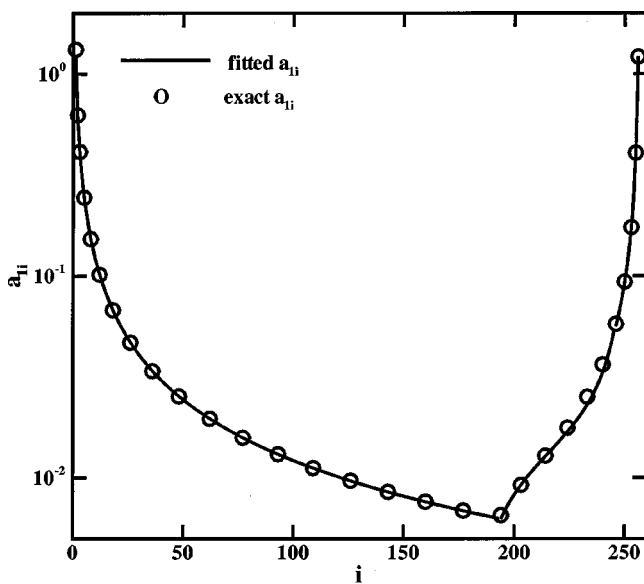


FIG. 2. Positive  $a_{1,i}$ 's resulting from an expansion of the kinetic distortion,  $F$ , in a basis of 512 Legendre polynomials. Approximate  $a_{1,i}$ 's may be generated using the following parameterizations:  $a_{1,1-194} = 1.233i^{-1.003}$ ,  $a_{1,195-245} = 9.50 \times 10^{-3} (1.0 - \tan[0.033(204 - i)])$ , and  $a_{1,246-256} = -1.86 \times 10^{-2} \tan[0.0305(205 - i)]$ .

electrons ( $2 < s < 4$ ) are responsible for carrying the heat flow in the collisional regime, the  $\bar{k}_i$ 's may be simplified to  $\bar{k}_i \approx k_i / (s^4 L_{\text{mfp}})$ , where  $Z_{\text{eff}} = 1$ . Performing the integrations over  $L$  and  $s$  yields

$$q_{\parallel} = - \frac{50}{3\sqrt{\pi}} n^{\text{eq}} v_{\text{the}} L_{\text{mfp}} \frac{\partial T}{\partial L} \sum_{\bar{k}_i > 0} \frac{|a_{1,i}|}{k_i} \approx - 11 \frac{n^{\text{eq}} T^{\text{eq}} \tau_e}{m_e} \frac{\partial T}{\partial L}. \tag{21}$$

This is Eq. (1) with a different numerical coefficient. The reason for the overshoot of about a factor of three may be explained as follows. The collisional analysis of Braginskii accounts for the full operator by using a moment approach that includes corrections due to momentum and heat flux restoring terms and finite flow, heat flow, and energy-weighted heat flow effects. In simpler terms, the error may partially be attributed to the fact that the Lorentz scattering operator ignores momentum loss of heat-flow-carrying electrons to the background plasma. In addition, energy loss and diffusion effects which push heat-flow-carrying electrons back into the background Maxwellian increase the effective collision frequency and reduce the heat flow by an estimated factor of 2–3. This is analogous to the reduction in electrical conductivity when going from the Lorentz to the Spitzer model.<sup>17</sup>

In order to write a form that is reminiscent of Eq. (2) we perform an integration by parts of Eq. (19) with respect to  $L$  which yields

$$q_{\parallel}(L') = \frac{n^{\text{eq}} v_{\text{the}}}{\pi^{3/2}} \int_0^{\infty} dL \frac{T(L' - L) - T(L' + L)}{L} \frac{\partial K}{\partial(\ln L)}. \tag{22}$$

This form of the closure resembles the collisionless flux of Eq. (2) with the additional term,  $\partial K/\partial(\ln L)$ , which contains the collisional information of a distribution of electrons as they scatter in pitch angle off a Maxwellian background plasma. It is important to point out that the expressions in Eqs. (19) and (22) yield the exact same result for arbitrary collisionality, thus either the temperature or its parallel gradient may appear in the integral operator. Figure 3 shows the falloff of the kernel  $(1/L)\partial K/\partial(\ln L)$  vs  $L$  compared with the kernel of the collisionless expression,  $2/L$ . The sharp falloff of  $(1/L)\partial K/\partial(\ln L)$  for  $L > 10$  is caused by collisions.

#### IV. HEAT FLOW FOR SINUSOIDAL TEMPERATURE PERTURBATION

In order to investigate the quantitative aspects of the closure stated in Eqs. (19) and (22), we examine the magnitude and nature of the heat flow for a sinusoidally varying temperature profile,

$$T(L) = T^{\text{eq}} - \tilde{T} \sin\left(\frac{2\pi L}{L_T}\right). \tag{23}$$

Here  $L_T$  represents the temperature gradient scale length. This temperature profile is a crude approximation to the tem-

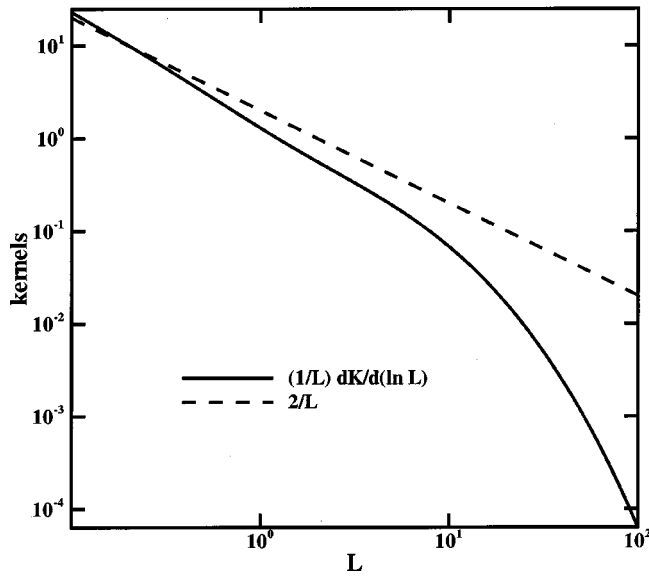


FIG. 3. The kernel  $(1/L)\partial K/\partial(\ln L)$  in Eq. (22) falls off faster than the kernel  $2/L$  from the collisionless expression in Eq. (2). Note the sharp falloff in  $(1/L)\partial K/\partial(\ln L)$  for  $L > 10$  due to collisions.

perature variations seen along a field line inside a helical magnetic island. Substituting the temperature profile into Eq. (22) and integrating over  $L$  yields

$$\begin{aligned} \bar{q}_{\parallel}(L') &= \left( \frac{\pi^{3/2}}{n^{\text{eq}} v_{\text{the}} \bar{T}} \right) q_{\parallel} \\ &= \frac{16\pi^2}{3} \int_0^{\infty} ds \left( s^2 - \frac{5}{2} \right)^2 s^3 e^{-s^2} \\ &\quad \times \sum_{\bar{k}_i > 0} \frac{|a_{1i}| L_T \bar{k}_i}{L_T^2 \bar{k}_i^2 + 4\pi^2} \cos\left( \frac{2\pi L'}{L_T} \right), \end{aligned} \quad (24)$$

where the dimensionless number of interest is  $L_{\text{mfip}}/L_T$  which appears in the expression  $L_T \bar{k}_i = (L_T/L_{\text{mfip}})[k_i/2s^4] \times (Z_{\text{eff}} + \Phi(s) - G(s))$ . In the analysis that follows we set  $Z_{\text{eff}} = 1$  and evaluate Eq. (24) at  $L' = 0$ .

We first investigate the convergence of the heat flux in Eq. (24) as eigenfunctions are added to the expansion. Figure 4 shows rapid convergence of  $\bar{q}_{\parallel}$  in the collisional limit ( $L_{\text{mfip}}/L_T \ll 1$ ), where collisions easily destroy the details of pitch-angle space. In the collisionless limit ( $L_{\text{mfip}}/L_T \gg 1$ ), 512 eigenfunctions are required to converge at  $L_{\text{mfip}}/L_T = 10^5$ . As expected, the fine-grained details of velocity space are not readily destroyed in nearly collisionless plasmas.

For the remainder of this section, we will compare  $\bar{q}_{\parallel}$  in Eq. (24) with  $N=512$  with the results predicted by Eqs. (1) and (2). Figure 5 shows that in the collisional regime, the general flux derived in this work displays the correct qualitative behavior with  $\bar{q}_{\parallel}$  increasing linearly with  $L_{\text{mfip}}/L_T$ . Note, however, that we overshoot the Braginskii flux for reasons that were discussed in the previous section. In the nearly collisionless limit, Eqs. (24) and (2) disagree by about a factor of  $\sqrt{2}$ . Despite a more rapid falloff with  $L/L_{\text{mfip}}$ , the heat flux in Eq. (24) has slightly larger contri-

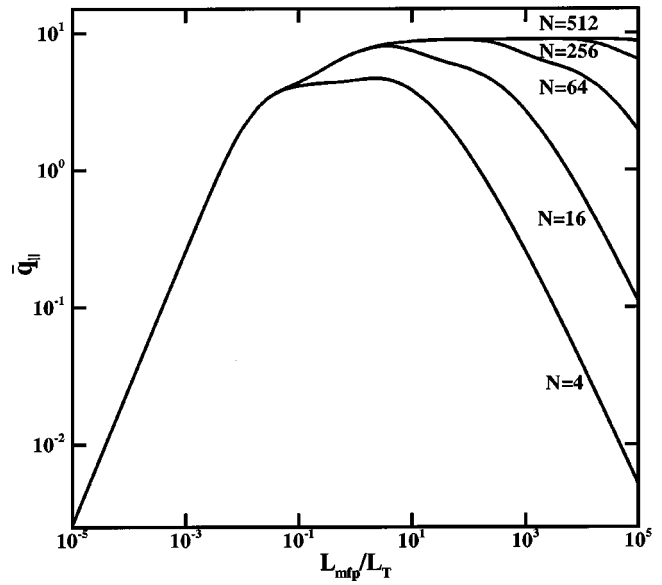


FIG. 4. Convergence of the heat flux  $\bar{q}_{\parallel}$  in Eq. (24) for a sinusoidal temperature perturbation in the nearly collisionless limit ( $L_{\text{mfip}}/L_T \gg 1$ ) as eigenfunctions are added to the expansion. For  $L_{\text{mfip}}/L_T = 10^5$ , convergence requires  $N=512$ . Convergence in the collisional limit ( $L_{\text{mfip}}/L_T \ll 1$ ) occurs with  $N$  as few as 2.

butions for  $L/L_{\text{mfip}} < 0.1$  (see Fig. 3). In the collisionless limit, Eq. (24) differs quantitatively from Eq. (2) due to the fact that time dependence was ignored prior to the solution of the set of equations generated by the expansion in pitch-angle eigenfunctions. Retaining time dependence along with the  $n=0$  coefficient equation brings the nearly collisionless heat flux presented here into quantitative agreement with the collisionless results given in Refs. 3 and 11.

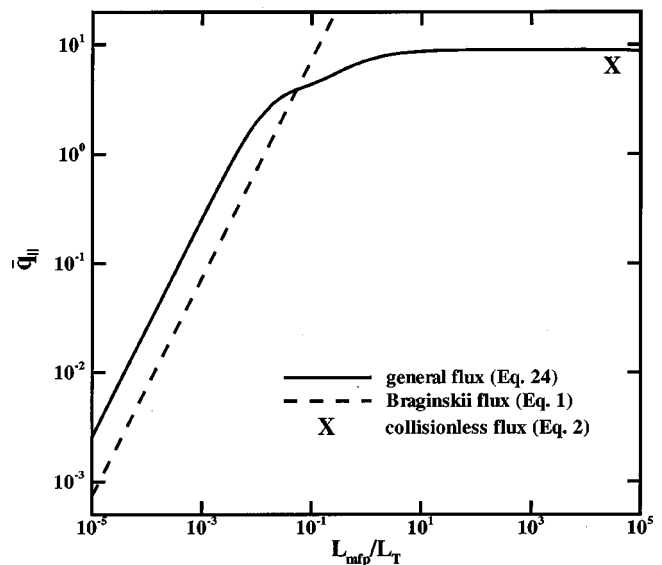


FIG. 5. In the collisional limit, heat flux in Eq. (24) yields correct qualitative behavior with  $\bar{q}_{\parallel}$  increasing linearly with  $L_{\text{mfip}}/L_T$ . The overshoot of the flux in Eq. (1) stems from the simple form for the collision operator used in deriving Eq. (24). In the nearly collisionless limit, Eqs. (24) and (2) disagree by about a factor of  $\sqrt{2}$ .

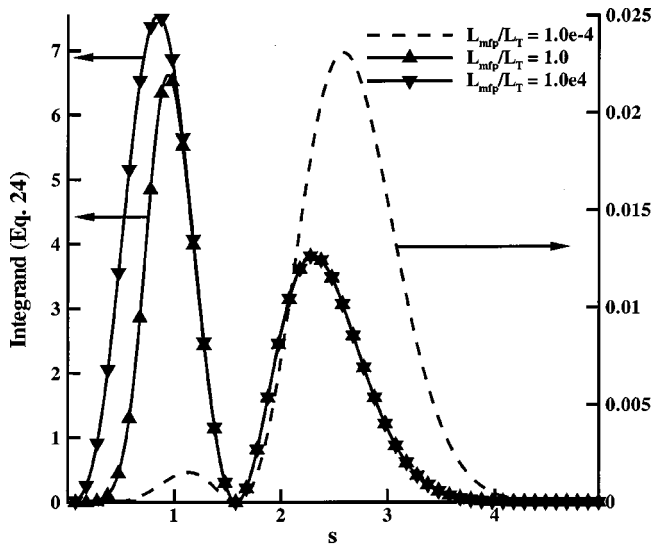


FIG. 6. Plot shows energy weighting of heat-flow-carrying electrons [integrand in Eq. (24)]. In the collisional regime ( $L_{mfp}/L_T = 10^{-4}$ ), higher energy electrons are responsible,  $s \sim 2-3.5$ . For moderate to low collisionalities ( $L_{mfp}/L_T = 10^0, 10^4$ ), thermal electrons are able to participate as the  $s^{-3}$  scaling in the collision frequency becomes less dominant.

In order to investigate the energy weighting of heat-flow-carrying electrons, we have plotted the integrand of Eq. (24) vs  $s$  in Fig. 6. It is assumed in this discussion that although including effects such as energy loss and diffusion in the collision operator may produce different quantitative results in regimes where collisions are important, the qualitative features of the weighting will remain the same. In the collisional limit ( $L_{mfp}/L_T = 10^{-4}$ ) we see that electrons with  $s \sim 2-3.5$  are dominant. It is interesting to note that the weighting of the heat flux in the collisional regime saturates with  $s \sim 2-4$  since for a nearly Maxwellian plasma the scarce number of tail electrons plays off against the  $s^3$  scaling of the heat flow moment and the  $s^{-3}$  scaling in the collision frequency. For moderate to low collisionality ( $L_{mfp}/L_T \sim 10^0-10^4$ ), thermal electrons play a more important role as the  $s^{-3}$  scaling in the collision frequency is less of a dominant factor in deciding which electrons can carry heat. Note that for all collisionalities there exists an important contribution to the heat flux from electrons with  $s \sim 2-3$ . This result is consistent with the observation of Krasheninnikov that electrons with energies,  $E \sim 4T^{eq} - 7T^{eq}$ , are responsible for heat flow in collisional to moderately collisional regimes.<sup>10</sup>

In order to emphasize the nonlocal nature of the closure written in Eqs. (19) and (22), we superpose two temperature perturbations with different gradient scale lengths, namely,

$$T(L) = T^{eq} - \tilde{T} \left[ \sin\left(\frac{2\pi L}{L_T}\right) + \sin\left(\frac{2\pi L}{10L_T}\right) \right]. \quad (25)$$

Figure 7 shows little change in the heat flow in the collisional case since electrons that were struggling to carry heat over the scale length,  $L_T$ , hardly recognize the additional scale length,  $10L_T$ . In regimes of moderate to low collisionality, however, the superposition of two gradient scale lengths approximately doubles the heat flow past  $L=0$ . It is

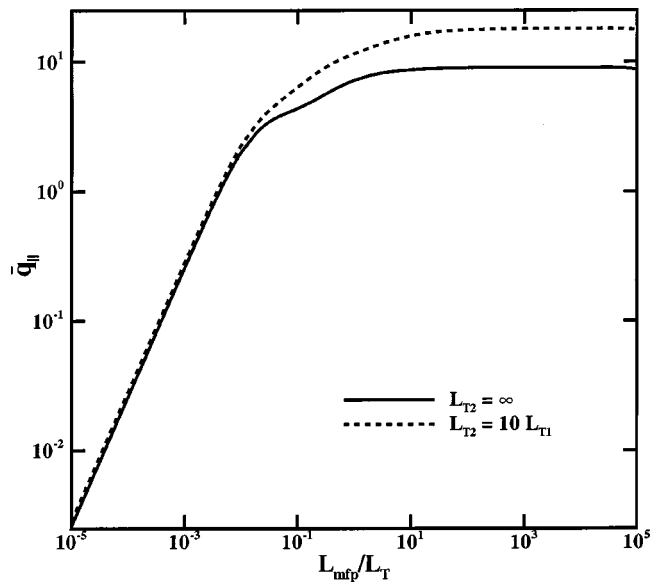


FIG. 7. An additional temperature perturbation of scale length  $L_{T2} = 10L_{T1}$  that is in phase with the original perturbation of Eq. (23) at  $L=0$  approximately doubles heat flow past  $L=0$  for moderate to low collisionalities. Only a slight increase is seen in the collisional regime.

important to emphasize that this doubling results from the fact that the temperature perturbations were chosen to be in phase at  $L=0$ . A  $\pi$  phase shift of the second perturbation relative to the first would lead to an approximate cancellation of the heat flow in the collisionless limit with only a slight reduction in the collisional limit.

Before leaving this section, we wish to emphasize the point that the parallel heat flux closure in Eqs. (19) and (22) allows for a continuous evolution in the physical nature of electron heat flow along magnetic field lines. In the collisional limit ( $L_{mfp}/L_T < 10^{-2}$ ), a local, diffusive process characterized by the random walk of suprathermal electrons dominates. In the collisionless limit ( $L_{mfp}/L_T > 10^2$ ), a non-local, free-streaming process characterized by the rapid motion of thermal and suprathermal electrons along field lines dominates. Although the limiting expressions and their interpretations are helpful guides to thinking about parallel transport, one should not assume that they represent the physics of conductive electron heat flow. In regimes of moderate collisionality, rather than interpreting the heat flow as partially diffusive and partially free-streaming, a better description attributes the heat flow to the random motion of a distribution of electrons as they travel along magnetic field lines and scatter in pitch-angle. Due to finite variations in electron temperature, these random parallel motions do not cancel and therefore yield a finite flow of heat. Such an interpretation holds for all collisionalities.

### V. HEAT FLOW ALONG A CHAOTIC FIELD

The subject of anomalous heat transport due to magnetic field line chaos has been of considerable interest as a means of explaining electron heat transport in magnetic fusion devices such as the reversed field pinch (RFP).<sup>7</sup> Although many previous authors infer an effective thermal diffusivity

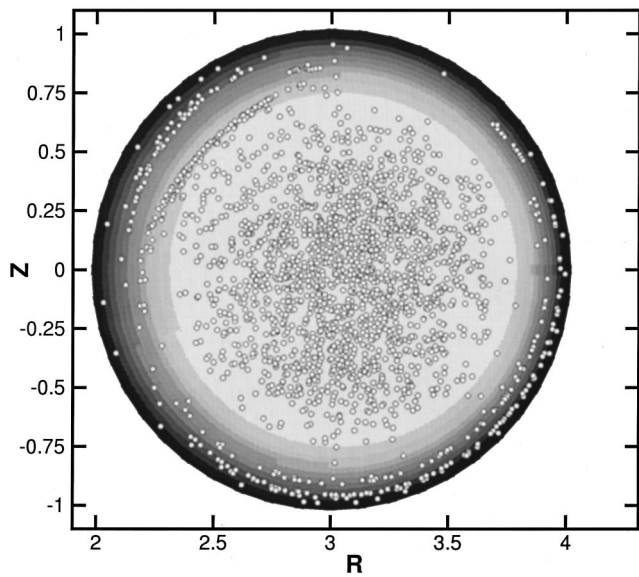


FIG. 8. Poincare surface of section showing field line chaos resulting from saturated tearing instabilities produced during a three-dimensional, zero-pressure RFP simulation. The chaotic field is superimposed on contours of constant electron temperature which were chosen to coincide with surfaces of constant, poloidal axisymmetric flux labeled by the variable  $\psi$ . Note that the field line chaos is confined primarily to the core where temperature is nearly flat.

based on the chaotic trajectories of thermal electrons,<sup>18,19</sup> here the flow of electron heat along a chaotic magnetic field is directly calculated using Eq. (22) and then translated into an effective thermal diffusivity. The goal here, however, is not to give a quantitative estimate of the cross-field thermal diffusivity since that requires additional physics such as electron trapping in  $|\mathbf{B}|$  wells and finite drift effects. Instead, we wish to emphasize the role played by the electron temperature profile and advocate the use of the general heat flux derived in this work as a means for attacking this problem. A quantitative analysis will be the subject of subsequent work.

For RFP's, a spectrum of tearing instabilities results in magnetic field line diffusivity that is responsible for electron temperature flattening inside of the reversal surface where the toroidal component of the magnetic field changes sign. Figure 8 shows a Poincare plot with chaotic field lines penetrating the poloidal plane. The magnetic field used to make this plot was the result of a three-dimensional, zero-pressure RFP simulation that was evolved to a nonlinearly saturated state using the magnetohydrodynamic code NIMROD.<sup>20</sup> Superimposed on the plot are contours of constant electron temperature that were chosen to correspond with surfaces of constant poloidal flux defined by the equilibrium and evolving axisymmetric field components. These surfaces of constant poloidal flux are labeled by the variable  $\psi$ . Inside the reversal surface where field line chaos dominates, we assume that the temperature profile is nearly flat. Outside the reversal surface, the temperature profile steepens. Note that because the temperature profile was not evolved but simply chosen to yield features similar to those seen in experiments, the results quoted below are strictly qualitative.

In order to define an averaged, effective radial ( $\nabla\psi$ )

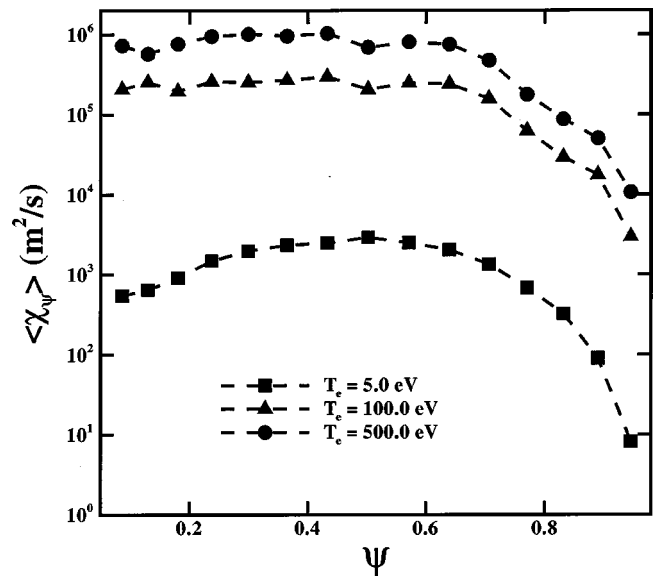


FIG. 9. Averaged effective cross-field electron heat diffusivity,  $\langle\chi_\psi\rangle$ , increases with on axis temperature,  $T_e=5.0, 100.0$ , and  $500.0 \text{ eV}$ . The  $\langle\chi_\psi\rangle$ 's were determined by averaging the radial component of the parallel heat flux calculated at 16 locations on a constant- $\psi$  surface.

thermal diffusivity,  $\langle\chi_\psi\rangle$ , we first determine the parallel heat flowing across the constant- $\psi$  surfaces as follows:

$$\mathbf{q}_\parallel \cdot \nabla\psi = -n^{\text{eq}} \chi_\psi \nabla T_e \cdot \nabla\psi. \quad (26)$$

Here the subscript  $\parallel$  refers to the total magnetic field (axisymmetric plus chaotic). The averaged thermal diffusivity may then be written

$$\langle\chi_\psi(\psi)\rangle = -\frac{1}{N} \sum_{i=1}^N \frac{\mathbf{q}_{\parallel i} \cdot \nabla\psi}{n^{\text{eq}}(\partial T_e / \partial \psi)_i (\nabla\psi)^2}. \quad (27)$$

Figure 9 shows  $\langle\chi_\psi\rangle$  for  $N=16$  plotted vs  $\psi$  for on-axis electron temperatures,  $T_e=5.0, 100.0$ , and  $500.0 \text{ eV}$ . As expected  $\langle\chi_\psi\rangle$  increases with decreasing collisionality as more mobile electrons become more efficient carriers of heat along chaotic field lines.

A more interesting result is shown in Fig. 10 which shows the 16  $\chi_\psi$ 's used to construct the  $\langle\chi_\psi\rangle$ 's in Fig. 9 on a constant- $\psi$  surface for  $T_e=500.0 \text{ eV}$ . Here electron heat occasionally flows against the local temperature gradient as evidenced by the finite number of negative  $\chi_\psi$ 's representing heat flowing radially inward. A collisional closure could only predict outward heat flow according to the local parallel gradient, thus missing the details of the temperature profile over longer scale lengths. On the other hand, a collisionless closure applied to present-day RFP's would overcompensate for the nonlocality by ignoring the natural truncation of the heat flux integral provided for by collisions. For these reasons, we advocate the use of the general heat flux closure in Eqs. (19) or (22) as a tool for studying electron heat transport in the presence of chaotic magnetic fields in the limit that  $|\mathbf{B}|$  variations and drift effects may be ignored.

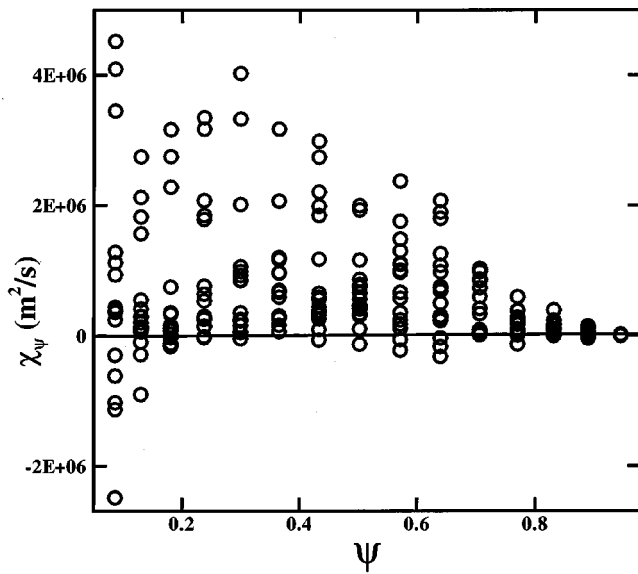


FIG. 10. Individual  $\chi_\psi$ 's used to calculate  $\langle\chi_\psi\rangle$  in Fig. 9 for  $T_e=500.0$  eV. Cases of parallel heat flowing against local temperature gradients correspond to  $\chi_\psi < 0$ .

**VI. CONCLUSIONS**

The parallel electron heat flux closure derived in this work takes the form of a generic integral operator involving electron temperature along a magnetic field line and the electron speed. Previously the collisional and collisionless heat fluxes have been interpreted as involving very different physics, namely, diffusion in the collisional limit and free-streaming in the collisionless limit. These processes represent limits of the unified physical behavior described in the following closure:

$$q_{\parallel} = -\frac{n^{\text{eq}}v_{\text{the}}}{\pi^{3/2}} \int_0^\infty dL \left[ \frac{\partial T(L'-L)}{\partial L} + \frac{\partial T(L'+L)}{\partial L} \right] K(L)$$

$$= \frac{n^{\text{eq}}v_{\text{the}}}{\pi^{3/2}} \int_0^\infty dL \frac{T(L'-L) - T(L'+L)}{L} \frac{\partial K}{\partial (\ln L)}, \quad (28)$$

where  $K(L)$  is defined in Eq. (20). It is important to reiterate that either the temperature or its parallel gradient may be used in the integral operator. Previous integral forms for the heat flux have only been written in terms of temperature.

In addition, the use of a speed-dependent, pitch-angle scattering operator permits a discussion of the energy weighting of heat-flow-carrying electrons. For all collisionalities, electrons with two to three times the thermal speed take part in carrying the conductive heat flow. This result

was observed previously for collisional to moderately collisional regimes. An additional bit of information provided by Eq. (28) is that thermal electrons are also responsible for carrying heat in nearly collisionless plasmas.

Finally, the usefulness of the general closure derived here was exhibited for the problem of electron heat transport in the presence of chaotic magnetic fields. The qualitative calculation revealed the need for a general heat flux capable of predicting the flow of electron heat against local temperature gradients. A quantitative calculation including complications due to drift effects and  $|\mathbf{B}|$  variations will be the subject of subsequent work.

**ACKNOWLEDGMENTS**

The authors would like to thank Dr. T. A. Gianakon, Dr. S. E. Kruger, and Dr. Y. Nishimura for many helpful discussions during the completion of this work. This research has been supported primarily by the DOE Fusion Energy Post-doctoral Research Program and the Computational Science Graduate Fellowship Program of the Office of Scientific Computing in the Department of Energy (DOE), and in part by U.S. DOE under Grant No. DE-FG02-86ER53218. The authors would also like to acknowledge the help of the NERSC support staff and the use of T3E computer time.

<sup>1</sup>S. I. Braginskii, *Transport Processes in a Plasma* (Consultants Bureau, New York, 1965).  
<sup>2</sup>G. W. Hammett and F. W. Perkins, *Phys. Rev. Lett.* **64**, 3019 (1990).  
<sup>3</sup>P. B. Snyder, G. W. Hammett, and W. Dorland, *Phys. Plasmas* **4**, 3974 (1997).  
<sup>4</sup>R. D. Hazeltine, *Phys. Plasmas* **5**, 3282 (1998).  
<sup>5</sup>R. D. Hazeltine, *Phys. Plasmas* **6**, 550 (1999).  
<sup>6</sup>B. D. G. Chandran and S. C. Cowley, *Phys. Rev. Lett.* **80**, 3077 (1998).  
<sup>7</sup>G. Fiksel, S. C. Prager, W. Shen, and M. Stoneking, *Phys. Rev. Lett.* **72**, 1028 (1994).  
<sup>8</sup>Z. Chang and J. D. Callen, *Phys. Rev. Lett.* **74**, 4663 (1995).  
<sup>9</sup>E. Gross and M. Krook, *Phys. Rev. Lett.* **102**, 593 (1956).  
<sup>10</sup>S. I. Krasheninnikov, *Phys. Fluids B* **5**, 74 (1993).  
<sup>11</sup>Z. Chang and J. D. Callen, *Phys. Fluids B* **4**, 1167 (1992).  
<sup>12</sup>Z. Chang and J. D. Callen, *Phys. Fluids B* **4**, 1182 (1992).  
<sup>13</sup>J. P. Wang and J. D. Callen, *Phys. Fluids B* **4**, 1139 (1992).  
<sup>14</sup>S. Chapman and T. G. Cowling, *The Mathematical Theory of Non-Uniform Gases* (Cambridge University Press, Cambridge, 1939).  
<sup>15</sup>R. D. Hazeltine and J. D. Meiss, *Plasma Confinement* (Addison-Wesley, Redwood City, 1992).  
<sup>16</sup>W. H. Press, S. A. Teukolsky, W. T. Vetterling, and B. P. Flannery, *Numerical Recipes in Fortran 77* (Cambridge University Press, New York, 1986).  
<sup>17</sup>L. Spitzer, *Physics of Fully Ionized Gases* (Wiley, New York, 1962).  
<sup>18</sup>A. B. Rechester and M. N. Rosenbluth, *Phys. Rev. Lett.* **40**, 38 (1978).  
<sup>19</sup>J. A. Krommes, C. O. Oberman, and R. G. Kleva, *Plasma Phys.* **30**, 11 (1983).  
<sup>20</sup>A. H. Glasser, C. R. Sovinec, R. A. Nebel, T. A. Gianakon, S. J. Plimpton, M. S. Chu, D. D. Schnack, and the NIMROD Team, *Plasma Phys. Controlled Fusion* **41**, A747 (1999).